

Enhanced Quantum Efficiency in UV light-Activated Ammonia Photodecomposition by Increasing Cell Volume and Concentration for Practical Use

Rie SAITO *² Hirohito UENO *¹ Junichi NEMOTO *¹
Yuki FUJII *¹ Akira IZUOKA *² Masao KANEKO *¹

Abstract

UV light-activated and highly efficient photodecomposition of high concentration ammonia that is a model compound of livestock and industrial wastewater, was successfully achieved with a high internal quantum efficiency by a combination cell composed of a nanoporous TiO₂ photoanode/O₂-reducing cathode unit and a large auto-oxidation chamber. In a vertical type submodule (reactor volume 21.8 L) irradiated by a solar simulator at the irradiance of 3.5mWcm⁻² UV light (1 sun condition), internal quantum efficiency η' reached over 500 (= 5 x 10⁴ %). It was found that enlarging the cell (wastes solution) volume brought about the increase of the quantum efficiencies, exhibiting that the UV photon density was not rate-determining, which was interpreted by the auto-oxidation of the photoactivated ammonia with original ammonia and O₂. The increase of the ammonia concentration enhanced the internal quantum efficiency almost linearly up to 10⁴ (= 10⁶ % at 1.9 M concentration), supporting also decomposition of photoactivated ammonia with original ammonia and O₂. A linear correlation of the η' with the ratio (=cm) of the cell volume cm³ vs. TiO₂ area cm² was obtained, which enables design of future large scale practical application of the present system.

Keywords: Biophotochemical Cell (BPCC) / nanoporous titanium dioxide photoanode/ O₂-reducing cathode/
Photodecomposition / Ammonia aqueous solution

1 Introduction

Photoelectrochemical reactions at semiconductor electrodes were investigated from before 1960s⁽¹⁻³⁾, and a crystalline n-TiO₂ photoanode to decompose water by UV light attracted a great attention⁽⁴⁾. Organic compounds have also been decomposed^(5,6). A nanoporous TiO₂ thin film was applied to a dye-sensitized solar cell (DSSC)⁽⁷⁾ in which a nanoporous TiO₂ film works in an organic liquid electrolytes solution while working as an electron acceptor and conductor rather than as a liquid-junction semiconductor. The photoreactivity of a nanoporous TiO₂ film has been an important issue towards applications in an aqueous phase. As

an application powders and coatings of semiconductors were used to photodecompose and clean environmental pollutants and dirty materials⁽⁸⁾. Since such so-called photocatalyst powders have to be adsorbed or coated onto a proper carrier material for practical use, their photocatalytic activity has not been high (usually limited to less than 100 to 1000 ppm pollutants) due to the hindrance against UV irradiation by the carrier materials as well as by the wastes. It has been not easy for conventional powder-based-photocatalysts utilizing only UV-light to clean a large volume of highly concentrated and colored pollutant solution due to the strong absorption of UV light by the carrier, solutes and solid suspensions. In order to increase photocatalyst's activity, narrow bandgap semiconductors capable of using visible light have been developed and achieved some success, but still the activity is not high enough. Environmental pollution by biowastes is becoming more and more a serious issue⁽⁹⁾, and among the pollutants, concentrated ammonia is one of the most serious industrial and biomass wastes, since ammonia is the second largest chemical products in the world. Moreover, livestock wastes such as pig urine that is quickly converted to ammonia

*¹ The Institute of Biophotochemonics Co.Ltd.
(2-1-1 Bunkyo, Mito, Ibaraki 310-8512, Japan)
e-mail: kaneko@biophotochem.co.jp

*² Faculty of Science, Ibaraki University
(2-1-1 Bunkyo, Mito, Ibaraki 310-8512, Japan)
(原稿受付: 2010年2月8日)

by urease abundant in nature are also serious pollutants. However, photocleaning of such concentrated and a large volume ammonia pollutants has been nearly impossible. The present authors reported a Biophotocatalytic Cell (BPCC) composed of a nanoporous semiconductor photoanode and an O_2 -reducing cathode that can photocatalytically decompose biomass and its wastes in water⁽¹⁰⁻¹³⁾. In the BPCC a nanoporous semiconductor thin film is exposed directly to the incident light, so that irradiation hindrance by concentrated solutes, colored compounds and suspended solids is almost negligible. We succeeded in remarkably enhancing the BPCC activity for ammonia photodecomposition with a nanoporous TiO_2 film photoanode / O_2 -reducing cathode attaining internal quantum efficiency (QE) over 100 ($=10^4$ %) in ammonia photodecomposition, exhibiting that the major decomposition of ammonia takes place by O_2 oxidation of the activated NH_3 by a kind of chain auto-oxidation mechanism^(14,15), which enabled photodecomposition of concentrated NH_3 pollutants over 10^4 ppm. It should be noted that NH_3 oxidation with O_2 is an exergic process allowing in principle spontaneous reaction, but activation is actually needed like combustion of fuels. In our ammonia photodecomposition system, photon is used to activate the NH_3 , and afterwards auto-oxidative chain reaction to N_2 takes place with high efficiency. We have further investigated that either enlarging the cell (wastes solution) volume or increasing the wastes concentration increased the quantum efficiencies remarkably, and the results will be reported here.

2. Experimental

2.1. Materials

Ti-nanoxide T/SP (particle size, 13nm; surface area, ~ 120 m²g⁻¹, anatase > 90%) was purchased from Solaronics Co. Ltd. Lead (II) acetate trihydrate (purity > 99.0%) and hydrogen hexachloro platinate (IV) hexahydrate (purity > 98.5%) were from Wako Pure Chemical Co. Ltd. F-doped SnO_2 conductive glass (FTO, surface resistance 10 Ω /sq) was purchased from AGC Fabritec Co. Ltd. As for the sample solution, an ammonia aqueous solution (28.0 % NH_3) was mainly used. The livestock wastewater sample that was a black-colored mixture of pig urine/wash water = 1/4 containing suspended solids (e.g. manure and pig bristles) was used by obtaining from a livestock breeding farmer house in Ibaraki prefecture, Japan.

2.2. Electrode preparation

A nanoporous TiO_2 film coated on an FTO electrode (FTO/ TiO_2) was prepared as before by a squeeze coating method, for which an adhesive tape (thickness about 70 μ m) was used as a spacer to adjust the TiO_2 film thickness

obtained after calcinations⁽¹⁷⁾. The TiO_2 film was at first dried at 100 °C for 30 min and then calcined at 450°C for 30min giving about 10 μ m thick film the roughness factor of which was nearly 10^3 . An O_2 reduction cathode was comprised of a stainless steel mesh (100mesh) coated at first by a thin layer of Nafion (cation exchange resin), and Pt black was electrodeposited thereafter (designated as SUS mesh/Pt-black).

2.3. Cell Fabrication

A cylindrical cell (Cell 1, 10mL, solution volume usually 5mL) was used to analyze the photodecomposition products under air-tight conditions. A thin layer type cell (Cell 2) was designed in order to minimize the solution resistance between the TiO_2 photoanode and the Pt-coated O_2 -reducing cathode, e.g., the solution layer thickness was usually adjusted to 5mm by using a spacer made of neoprene rubber put between a 6cm x 6cm (effective area = 5cm x 5cm) size photoanode (TiO_2 film) and an O_2 -reducing Pt cathode. Stainless steel (SUS) foil charge collectors with 5mm wide were put on the four edges of the FTO conducting layer both on the anode and the cathode in contact with the spacer.

An efficient Cell 3 (Fig.1, 250mL) was designed and fabricated by combining the fundamental thin layer structure of the Cell 2 unit using a Pt-black coated SUS mesh cathode with a large volume of solution chamber where auto-oxidation of the activated compounds takes place.

A quasi-submodule Cell 4 (3.26L) is shown in Fig.2, which consists of a photoanode/cathode unit and a much larger volume reaction chamber than that of the Cell 3. The large reaction chamber of 15 cm x 15 cm x 15cm was made of a 1 cm thick poly(methylmethacrylate) plate. A vertical type Cell 4 in which a photoanode/cathode unit is located on the top of the cell was designed so as to irradiate the TiO_2 film from the top. For this cell the chamber volume was changed from 190mL to 3260mL by using acrylic-blocks put in the solution phase as shown in Fig.2 a).

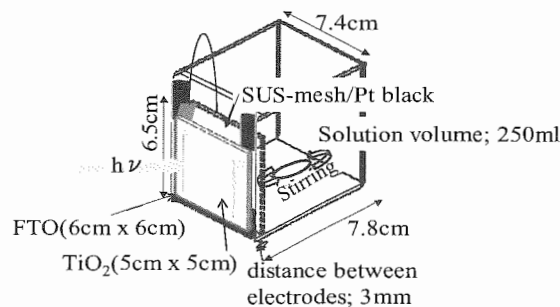


Fig.1. Combination cell (Cell 3) comprising a photoanode/cathode unit and a bulk reaction chamber.

times as much as the AM1 that is the spectral distribution of

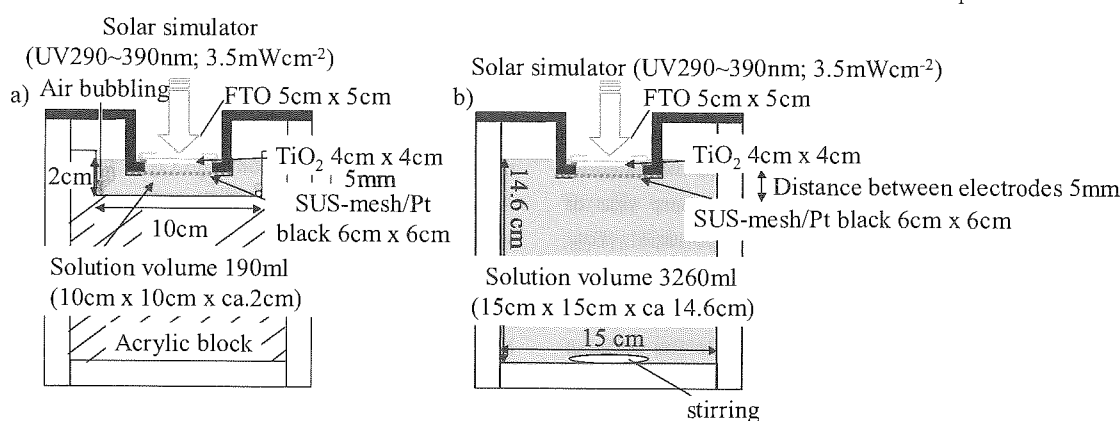


Fig. 2 Sectional view of a vertical type quasi-submodule (Cell 4) comprising a photoanode/cathode unit and a bulk reaction chamber. Liquid volume; a) 190mL, b) 3260mL.

A vertical type submodule (Cell 5, 21.8 L) consists of a larger photoanode/cathode unit and a much larger bulk reaction chamber than that of the Cell 4. The photoanode and the cathode separated at the distance of 3 mm consist of an FTO/TiO₂ (10 cm x 10cm, effective area 9cm x 9cm) and the SUS mesh/Pt-black cathode (10cm x 10cm). This submodule was 21cm x 21cm x 60cm size made of a poly(methylmethacrylate) plate with the solution volume of 21cm x 21cm x 50cm (21.8L) as shown in Fig.3.

2.4. Irradiation and measurements

The UV-A region light intensity was measured by a UV light meter (model UV-340, CUSTOM Co. Ltd.). The TiO₂

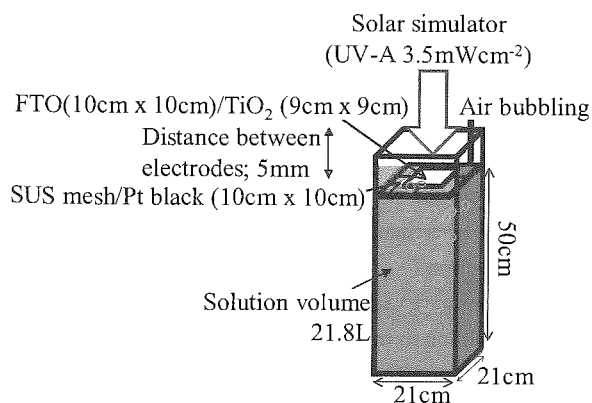


Fig. 3 A sub-module (Cell 5) comprising a photoanode/cathode unit and a bulk reaction chamber. Liquid volume, 21.8L.

film was irradiated at 100mWcm⁻² white light with a 500W xenon lamp through an IR-cutoff filter (HA-50), which contained UV-A (290-390nm) region light with the intensity of 8mWcm⁻². This UV intensity was the same as that from a solar simulator (PEC-L10 from Peccell Technologies, Inc.) at the total irradiance of AM 1.5 G and 100mWcm⁻². AM1.5G is a standard irradiation spectral distribution, and AM1.5 means that solar irradiation passed through the air whose mass is 1.5

the solar irradiation on the sea level when the sun irradiates vertically. The Cells 4 and 5 were irradiated with the UV light intensity of 3.5mWcm⁻² (1 sun condition) from a solar simulator. As a reference, the UV irradiance on a sunny day of Oct. 28th at 14:50 in our campus was 4.5mWcm⁻² when the total solar irradiance was 100mWcm⁻². The incident photon (on the FTO) to current conversion efficiency (IPCE) was measured by a Cell 2 type composed of a 2cm x 2cm photoanode and a cathode (each effective area was 1cm x 1cm) under irradiation by a monochromatic light of 350nm (Shimadzu-Bausch & Lomb monochromator).

The N₂ formed in a cylindrical cell (Cell 1) was analyzed by a gas chromatograph (Shimadzu, GC-8A and GC-2014) with a molecular sieve 5A column at 30°C using Ar carrier gas, and CO₂ by a silica gel column at 80°C using He carrier gas. For calculating the amount of the total formed CO₂, the gas volume in the gas phase was corrected by its solubility in water. All the photoelectrochemical reactions were performed at 25°C. NH₄⁺, NO₂⁻ and NO₃⁻ were analyzed by a DR2800 analyzer from Hach Company, USA.

During the photoelectrochemical reactions, time dependence of the short circuit photocurrent was measured by a potentiostat/galvanostat (HA-301, Hokuto Denko), a function generator (HB-104, Hokuto Denko) and a coulomb/amperehour meter (HF-201, Hokuto Denko).

3. Results and Discussion

The photoelectrochemical reactions in a BPCC composed of a nanoporous semiconductor photoanode and an O₂-reducing cathode for decomposition of biomass and its model compounds to produce CO₂ and N₂ have been established in our previous papers⁽¹⁰⁻¹³⁾. Also in the present NH₃ photodecomposition, the product (N₂) was analyzed by the cell 1. As known well in a liquid-junction semiconductor photoelectrochemical system⁽¹⁻⁵⁾, excitation of electrons from

the valence band (VB) to the conduction band (CB) takes place by irradiation of a semiconductor photoanode with the light whose energy is larger than the bandgap of the semiconductor, forming separated holes in the VB and electrons in the CB, and thus separated charges induce oxidation and reduction at the photoanode and the cathode, respectively. A nanoporous TiO₂ showed a sharp rise of anodic photocurrent around the CB edge potential (E_{CB} , -0.77V vs. SHE at pH 12⁽¹⁶⁾) reaching rapidly an equilibrium photocurrent in its cyclic voltammogram (CV) in an NH₃ aqueous solution under UV irradiation⁽¹⁰⁾. On the basis of this CV and a clear photovoltage–photocurrent characteristics with a high Fill Factor (0.65), it was concluded that the nanoporous TiO₂ forms a kind of Schottky junction (liquid–junction) with the aqueous ammonia^(10,17). In our previous papers, UV light-activated and efficient photodecomposition of an ammonia aqueous solution was achieved to produce dinitrogen (N₂) with high internal quantum efficiency ($= \eta'$) over 300⁽¹⁸⁾ by a BPCC comprising a nanoporous semiconductor film photoanode/O₂-reducing cathode unit and a large bulk reaction chamber, where the internal quantum efficiency for the decomposition ($= \eta'$) is defined as the ratio of the total decomposition number against photon number effectively used for activating the substrate (shown later in eq.1). It was shown that a BPCC composed of a photoanode/cathode unit and large volume reaction chamber is effective as an efficient cell.

The Cell 3 (Fig.1) was designed so as to provide a large reactor volume (250mL) in combination of a BPCC photoreaction center unit comprising a nanoporous TiO₂ photoanode and an O₂-reducing cathode that are placed close with each other at the position facing directly the incident

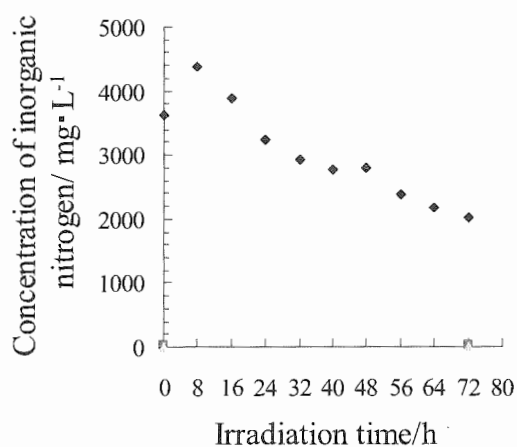


Fig.4 Changes of NH₄-N nitrogen with time in the photodecomposition of a 250mL mixture of pig urine and 4 times wash water in the Cell 3 (see Fig.1) under stirring and 8mWcm⁻² UV irradiation. Symbols: ◆ NH₄-N, ■ NO₂-N, ○ NO₃-N.

light. A stainless steel mesh coated by a Nafion polymer thin film and electrodeposited Pt-black was used as an O₂-reducing cathode such that the activated biomass intermediates can diffuse from the TiO₂ nanopores into the large volume of the bulk solution through the cathode mesh to undergo dark chain reaction with O₂ in the reaction chamber. A 250 mL of black-colored pig urine mixture with 4 times volume of water whose initial NH₄-N content was 3620ppm (NH₄⁺ = 258mM) was magnetically stirred and irradiated with 100mWcm⁻² white light (UV light 8mWcm⁻²). This sample has about 2.6 times higher initial ammonium nitrogen concentration than the previously reported pig urine⁽¹⁵⁾, and additionally, twice higher initial organic nitrogen concentration in the forms of protein, amino acid and urea⁽¹⁵⁾. In the photodecomposition of NH₄⁺ in this pig urine/water mixture, the changes of NH₄-N with irradiation time are shown in Fig.4, including the NO₂-N and NO₃-N concentration data at start and after 72h.

In the first 8h NH₄-N was increased, which can be attributed to the formation of NH₃ by the photodecomposition of urea by urease contained usually in pig urine, and thereafter NH₄⁺ was decreased by photodecomposition. The NH₄-N decomposition ratio was 44.1% after 72h, organic nitrogen was decreased from 980 to 672 mg/L (31.4% decrease) and BOD from 4400 to 1870 mg/L (57.6% decrease). In addition to this, it is important in the Fig.4 that NO₂-N and NO₃-N, serious eutrofication pollutants, did not increase. It should be noted here that ammonia is converted mainly to N oxides when powder-based TiO₂ was used to photodecompose ammonia.

In the present BPCC, since the TiO₂ thin film forms a clear Schottky-type junction with an aqueous ammonia solution^(10,17), the charges passed through the external circuit can be regarded nearly equal to the amount of the charges used effectively for substrate oxidation at TiO₂^(14,15), so that it is possible to estimate the internal quantum efficiency for the decomposition ($= \eta'$) (eq. 1), that is, the denominator in the eq.1 is estimated from the charges passed at the external circuit. In addition to the internal quantum efficiency η' , the external quantum efficiency (η), quantum efficiency of the reaction number based on total incident UV photon number, was obtained by using the incident photon to current efficiency = IPCE (eq. 2). The intrinsic quantum efficiency (η''), quantum efficiency of the reaction number against the UV photon number absorbed by the TiO₂ film, was obtained by measuring the UV photon number absorbed by TiO₂ film (eq. 3).

$$\text{Internal quantum efficiency, } \eta' =$$

decomposed mol of substrate x number of electron involved in one molecular decomposition / photon number in mol effectively used for activating the substrate (1)

$$\text{External quantum efficiency, } \eta = \eta' \times \text{IPCE} \quad (2)$$

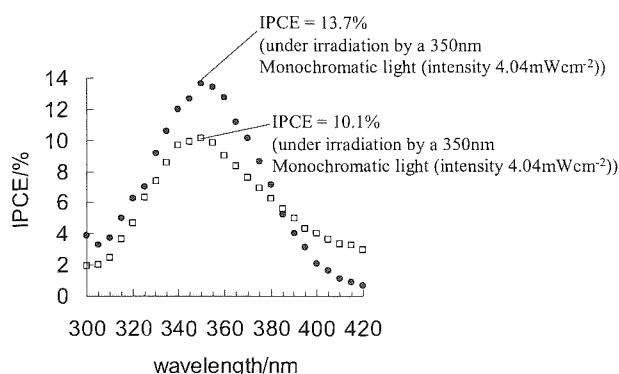


Fig.5 IPCE of ammonia aqueous solution and pig urine. Symbols: ● NH₃ aq (NH₄⁺; 65mM = NH₄-N; 910mg/L), □ mixture of pig urine and wash water (NH₄⁺; 258mM = NH₄-N; 3620mg/L)

pig urine (NH₄-N = 3620ppm, NH₄⁺ = 258 mM) was investigated and the action spectrum is shown in Fig.5 giving the IPCE of 10.1%. Although pig urine was strongly black-colored and involved suspended solids, the IPCE curve showed a clear maximum at 350nm that is the peak position of the irradiated monochromatic light. Since the TiO₂ film is directly exposed to the incident UV light in a BPCC, the strong light absorption by the sample liquid and the solid suspensions did not inhibit the effective UV irradiation on the TiO₂. In this Fig. 5 the IPCE for a 65mM NH₃ aqueous solution is also shown (IPCE = 13.7%) in order to be used in the Tables 2 and 3 described later.

After 72h, 44.1% NH₄⁺ was oxidatively decomposed that corresponds to the charges of 8.25 x 10³ C. During this

Table 1 Photodecomposition of 250mL mixture of pig urine and 4 times wash water (initial NH₃=103mmol) in the combined cell for 72 h (Cell 3, Fig.1) with a Xe lamp at 100mWcm⁻² intensity

Initial NH ₄ -N /mg·L ⁻¹ (NH ₄ ⁺ ; mM)	Final NH ₄ -N /mg·L ⁻¹ (NH ₄ ⁺ ; mM)	Decomposition of NH ₃ ratio/%	Coulombs corresponding to NH ₃ decomposition (b)/C	Coulombs passed (a)/C	η' (=b/a)	η (=η' x IPCE)	η''
3620 (258)	2020 (144)	44.1	8.25 x 10 ³	213	39	3.9	7.3

Table 2 Photodecomposition of an ammonia aqueous solution (initial NH₃=55.7mmol for 190mL sol. and 848mmol for 3260mL) in the quasi-submodule vertical type combination cell (Cell 4, Fig.2) with a solar simulator under AM 1.5G (UV region 3.5mWcm⁻²) in 6h.

Soln. Vol./mL	Initial NH ₄ -N /mg·L ⁻¹ (NH ₄ ⁺ ; mM)	Final NH ₄ -N /mg·L ⁻¹ (NH ₄ ⁺ ; mM)	Decomposition of NH ₃ ratio/%	Coulombs corresponding to NH ₃ decomposition (b)/C	Coulombs passed (a)/C	η' (=b/a)	η (=η' x IPCE)	η''
190	4110 (293)	1670 (119)	59.4	9.57 x 10 ³	51	188	26	6.7
3260	3640 (260)	3470 (248)	4.80	11.8 x 10 ³	38	310	42	11

Table 3 Photodecomposition of an ammonia aqueous solution (initial NH₃=3030mmol) in the submodule vertical type combined cell (Cell 5) for 6 h with a solar simulator under AM 1.5G (UV region 3.5mWcm⁻²).

Soln. Vol./mL	Initial NH ₄ -N /mg·L ⁻¹ (NH ₄ ⁺ ; mM)	Final NH ₄ -N /mg·L ⁻¹ (NH ₄ ⁺ ; mM)	Decomposition of NH ₃ ratio/%	Coulombs corresponding to NH ₃ decomposition (b)/C	Coulombs passed (a)/C	η' (=b/a)	η (=η' x IPCE)	η''
21800	1950 (139)	1810 (129)	7.19	63.2 x 10 ³	119	532	73	19

Intrinsic quantum efficiency, η'' = decomposed mol of substrate x number of electron involved in one molecular decomposition / absorbed photon mol by TiO₂ (3)

The IPCE measurement using the Cell 2 (nanoporous TiO₂ film, effective area 1cm x 1cm) was performed for the estimation of the external quantum efficiency. The IPCE of

photodecomposition time, 213 C charges were passed at the external circuit. Therefore, the internal quantum efficiency η' was 8.25 x 10³C/213C = 39 and the external quantum efficiency η was calculated to be 39 x 0.10 = 3.9. These results are shown in Table1. Additionally, the FTO conducting glass transmitted 60% of the incident UV light, and the absorption by the TiO₂ film was measured to be 88% of the

UV light transmitted through the FTO, so that the TiO₂ film alone absorbed 53% (= 60% x 88%) of the total incident UV light. Therefore, APCE (= absorbed photon to current efficiency) = IPCE/0.53, so that η'' is represented by $\eta' \times$ APCE = $\eta' \times$ (IPCE/0.53). Therefore, intrinsic quantum efficiency η'' was calculated to be $39 \times (0.10/0.53) = 7.3$.

Another type Cell 4 having a vertical cell structure that is more practical for utilizing solar irradiation was fabricated. Photodecomposition of an ammonia aqueous solution was investigated as a livestock waste model compound by disappearance of NH₄⁺ under magnetic stirring or air bubbling by solar simulator irradiation (AM 1.5, 75mWcm⁻² total irradiance in which UV light was 3.5mWcm⁻²). Our previous report showed that the total decomposed NH₃ increased linearly with the solution volume by increasing the reactor (solution) volume with the Cell 3 due to the favorable oxidative decomposition of the activated ammonia with O₂ by a kind of chain mechanism in the large chamber⁽¹⁸⁾. It means that the main decomposition reaction takes place in the large volume chamber independent of the photoirradiation. Therefore, the chamber volume of Cell 4 was changed from 190 to 3260ml by utilizing poly(methyl methacrylate) blocks as shown in Fig.2, and the quantum efficiencies for the NH₃ decomposition were investigated. It was confirmed that the same IPCE value as before (13.7%) is applicable also to this concentration, and the results are shown in Table 2. It should be noted that the quantum efficiencies increased by about 1.6 times with the increase of the reaction volume by 17 times demonstrating that the incident photon density is not yet rate-determining, but the oxidative decomposition with O₂ is the major process.

In order to see the effect of the cell (solution) volume, the cell size was enlarged by 6.7 times from the Cell 4 to the Cell 5 (21.8 L). In the photodecomposition of a 139 mM NH₃ aqueous solution in the vertical type submodule (Cell 5, 21.8 L) under air bubbling and at 3.5mWcm⁻² UV irradiance (with a solar simulator), the changes of NH₄⁺ with irradiation time were investigated. Air bubbling was conducted to stir the solution, so that the amount of air passed was not high, the ammonia decomposition efficiency being similar to the one conducted only with stirring. It should be added here that air bubbling can bring about evaporation of ammonia; the details are now under study, and will be reported elsewhere. After 6 h 7.19% NH₄⁺ was decomposed corresponding to decomposition by 63.2 x 10³C, while 119 C passed at the outer circuit, exhibiting that the internal quantum efficiency η' was $63.2 \times 10^3 \text{C} / 119 \text{C} = 532$, much higher than the quasi-submodule vertical type Cell 4. The external quantum efficiency η was calculated to be $532 \times 0.137 = 73$, and intrinsic quantum efficiency η'' was calculated to be $73 \times (0.137/0.53) = 19$. These results are shown in Table 3. It is important in this Table 3 that the quantum efficiencies

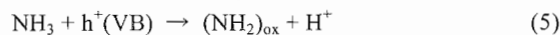
increased still by increasing the solution volume.

The mechanism of the photodecomposition of ammonia with high quantum efficiency was already reported in our previous papers, but it is shown again here by the equations from (4) to (7).

(Anodic reaction)



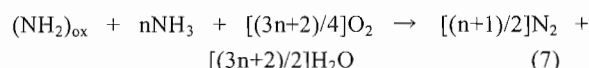
Activation of ammonia at photoanode:



(Cathodic reaction)



Auto-oxidative chain reaction of (NH₂)_{ox} with NH₃ and O₂ in the bulk chamber:



The nanostructured TiO₂ film photoanode forms a kind of Schottky junction with the ammonia aqueous solution, which induces charge separation by absorbing the UV light whose wavelength is shorter than 390 nm (eq.4). Ammonia is oxidized by the hole in the valence band (VB) to form an unstable oxidized intermediate (NH₂)_{ox} (eq. 5). The (NH₂)_{ox} would be oxidized rapidly with O₂ by a chain auto-oxidation mechanism, during which n x NH₃ molecules would be activated by active intermediate by a kind of chain reaction mechanism (eq.7) where n is equal to $\eta' - 1$. The structure of (NH₂)_{ox} is not known yet, but it can be hydrazine (H₂N=NH₂) and/or hydroxyl amine (NH₂OH) that are highly reactive with O₂. The chain auto-oxidation mechanism involving (NH₂)_{ox}, NH₃, and O₂ is also not yet known; it is the subject to be investigated further. The electrons in the conduction band (CB) would mainly be transported to the cathode due to the Schottky junction and be accepted by O₂ to directly form H₂O or via H₂O₂ to finally form H₂O (eq. 6). Fig. 6 represents such efficient photodecomposition of ammonia in a combination

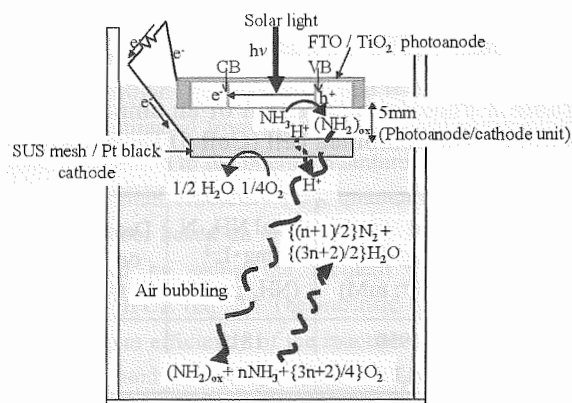


Fig.6 Photodecomposition mechanism of ammonia in a combination cell comprising a photoanode/cathode unit and a large bulk reaction chamber. The mechanism comprises activation of substrates by UV light at the photoanode/cathode unit and auto-oxidation of the activated substrates with NH₃ and O₂ (main decomposition) in the large chamber.

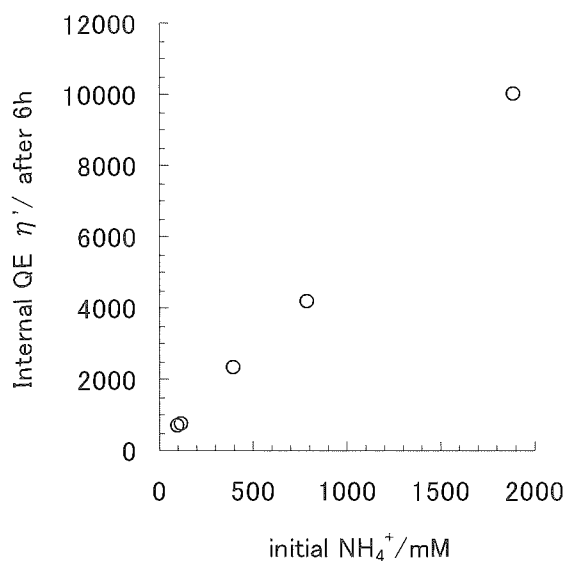


Fig.7 Internal quantum efficiency for photodecomposition (η') in a Cell 3 against initial ammonia concentration (mM) under 6h's irradiation. Reactor chamber volume; 250mL.

cell composed of a photoanode/cathode unit and a large auto-oxidation chamber.

It is important in the combination cell that the major decomposition reaction is dark auto-oxidation of the activated ammonia by the bulk O_2 , the internal quantum efficiency exceeding 500⁽¹⁸⁾. If the auto-oxidation mechanism shown in the eq.(7) is right, the quantum efficiency must be higher when the ammonia concentration is higher. In order to prove this, the initial concentration of ammonia was changed from 100mM to 1890mM, and the photodecomposition of an NH_3 aqueous solution was investigated in the Cell 3 (solution volume 250mL). It was found that the total decomposed NH_3 increased linearly with the initial ammonia concentration. The internal quantum efficiency η' was calculated and is shown in Fig.7 against NH_3 concentration, exhibiting a linear increase of η' with the concentration. When the initial concentration was 1892mM NH_3 , η' reached a very high value of 10016 (= ca. 10^6 %) supporting that the major decomposition mechanism can be represented by the eq.(7).

Finally, submodule should be further scaled up for future practical use. Since it can strongly be suggested from our previous^(14,15,18) and the present results that the internal quantum efficiency (η') must be closely correlated with the ratio of the cell volume and TiO_2 area ($\text{cm}^3/\text{cm}^2=\text{cm}$). The η' values against this ratio were taken from the Tables 1, 2 and 3, and plotted in the Fig. 8 (open circles), where the plot near the origin comes from the fact that η' approached 1 when the cell volume became much smaller. Although the plots were rather scattered probably due to the different cell structure and ammonia concentration, the η' value showed a clear linear correlation with the (cell volume/ TiO_2 area ratio) (cm). This result demonstrates that this ratio must be the

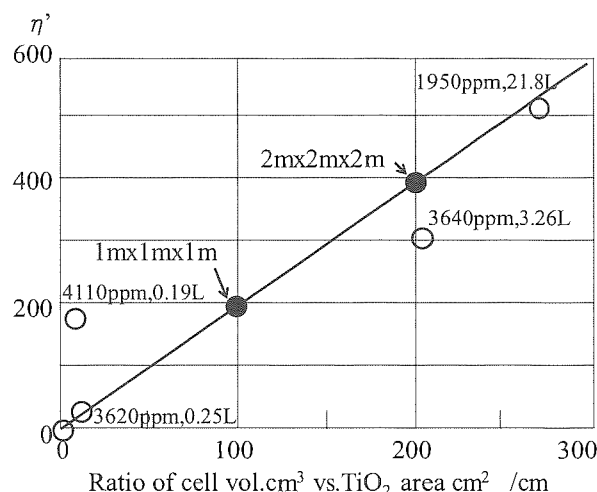


Fig.8 Internal quantum efficiency (η') (○) against the ratio (cm) of liquid volume / TiO_2 area, taken from the data of Tables 1~3, as well as the estimated η' (●) for 1m^3 and 8m^3 modules. Ammonia concentration (ppm) and cell volume (L) are indicated at the plots.

predominant factor to determine the cell activity, and that this linear correlation could be used to design a larger size module.

As an example, when 1m^3 (=1m x 1m x 1m) module with 1m^2 TiO_2 film area (volume/film area = 1m = 100 cm) was used, η' is estimated to be 200 (closed plot) from the line of Fig.8. When the module size is 8m^3 (=2mx2mx2m), the ratio, volume/ TiO_2 area, is $8\text{m}^3/4\text{m}^2=200\text{cm}$, for which η' is obtained to be 400. This shows that the 250mL laboratory cell results can be applied to the efficiency of much larger modules. When adopting the Tab.3 reaction conditions ($\text{NH}_3=139\text{mM}$, irradiance = $3.5\text{mWcm}^{-2}\text{UV}$), $\eta = \eta' \times \text{IPCE} = 200 \times 0.137=27.4$. The irradiance is about 1×10^{-8} mol photons $\text{cm}^{-2}\text{s}^{-1}$ if assuming the irradiated wavelength centered at 350 nm, which corresponds to 0.36 mol photons $\text{m}^{-2}\text{h}^{-1}$. This implies that 139 mol NH_3/m^3 (= $139 \times 3=417$ mol e^-/m^3) is decomposed by 0.36 mol photons/h with external quantum efficiency (η) of 27.4, which gives 417 mol $\text{e}^-/(0.36\text{mol photons h}^{-1} \times 27.4) = 42\text{h}$ reaction time for complete photodecomposition when assuming a linear decomposition correlated with time. Since the decomposition rate would be slowed down at final stage of the reaction, around 60 h would probably be needed to attain more than 90% photodecomposition, and therefore when taking 6 h's solar irradiation per day at average $3.5\text{mWcm}^{-2}\text{UV}$, 10 days should at least be needed for more than 90% photodecomposition. This estimation shows that when 10 pieces of 1m^3 module are used, 1m^3 of 139 mM NH_3 wastewater per day could be treated and cleaned in one day by solar irradiation.

It should be added finally about industrial and livestock wastewater. There have been no good methods to treat and

clean such wastewater containing concentrated ammonia. The present reported method is simpler and more efficient than any existing methods, which could promise near future practical application.

4. Conclusions

UV light-activated and highly efficient photodecomposition of high concentration ammonia that is a model compound of livestock and industrial wastewater, was successfully achieved with a high internal quantum efficiency by a combination cell composed of a nanoporous TiO₂ photoanode/O₂-reducing cathode unit and a large auto-oxidation chamber. In a vertical type submodule (reactor volume 21.8 L) irradiated by a solar simulator at the irradiance of 3.5mWcm⁻² UV light (1 sun condition), internal quantum efficiency η' reached over 500 (= 5 x 10⁴ %). It was found that enlarging the cell (wastes solution) volume brought about the increase of the quantum efficiencies, exhibiting that the UV photon density was not yet rate-determining, which was interpreted by the auto-oxidation of the photoactivated ammonia with starting ammonia and O₂. The increase of the ammonia concentration enhanced the internal quantum efficiency almost linearly up to 10⁴ (= 10⁶ % at 1.9 M concentration), supporting also decomposition of photoactivated ammonia with original ammonia and O₂. A quasi-linear correlation of the η' with the ratio (=cm) of the cell volume cm³ vs. TiO₂ area cm² was obtained, which enables design of future large scale practical application of the present system.

Acknowledgment

The present work was partially supported by the Project for Water Environment Renovation of Lake Kasumigaura in the Science and Technology Promotion Foundation of Ibaraki.

5. References

- (1) H. Gerischer, *Z. Phys. Chem.* 26 (1960) 325.
- (2) H. Gerischer, H. Tributsch, *Ber. Bunsenges. Phys. Chem.* 72 (1968) 437.
- (3) H. Tributsch, H. Gerischer, *Ber. Bunsenges. Phys. Chem.* 73 (1969) 850.
- (4) A. Fujishima, K. Honda, *Nature* 238 (1972) 37.
- (5) R. W. Matthews, in: E. Pelizzetti, M. Schiavello (Eds.), *Photochemical Conversion and Storage of Solar Energy*, Kluwer Academic Publishers, Dordrecht, 1991, pp. 427-449.
- (6) M. Kaneko, I. Okura (Eds.), *Photocatalysis -Science and Technology-*, Kodansha/Springer, Tokyo, 2002.
- (7) B. O' Regan, M. Graetzel, *Nature* 353 (1991) 737.
- (8) A. Fujishima, K. Hashimoto, T. Watanabe, *TiO₂ Photocatalysis -Fundamental and Applications-*, BKC Inc., Tokyo, 1999.
- (9) C. J. Stevens, N. B. Dise, J. O. Mountford, D. J. Gowing, *Science* 303 (2004) 1876.
- (10) M. Kaneko, J. Nemoto, H. Ueno, N. Gokan, K. Ohnuki, M. Horikawa, R. Saito, T. Shibata, *Electrochem. Commun.* 8 (2006) 336.
- (11) J. Nemoto, M. Horikawa, K. Ohnuki, T. Shibata, H. Ueno, M. Hoshino, M. Kaneko, *J. Appl. Electrochem.* 37 (2007) 1039.
- (12) M. Kaneko, H. Ueno, K. Ohnuki, M. Horikawa, R. Saito, J. Nemoto, *Biosens. Bioelectron.* 23 (2007) 140.
- (13) T. Okada, M. Kaneko (Eds), *Molecular catalysts for energy conversion*, Springer Verlag, Berlin, 2008.
- (14) M. Kaneko, H. Ueno, R. Saito, J. Nemoto, *Cat. Lett.*, 131 (2009) 184.
- (15) M. Kaneko, H. Ueno, R. Saito, S. Yamaguchi, Y. Fujii, J. Nemoto, *Appl. Cat., B:Environmental* 91 (2009) 254.
- (16) A. Hagfeldt, M. Graetzel, *Chem. Rev.* 95 (1995) 49.
- (17) H. Ueno, J. Nemoto, K. Ohnuki, M. Horikawa, M. Hoshino, M. Kaneko, *J. Appl. Electrochem.*, 39 (2009) 1897.
- (18) R. Saito, H. UENO, J. Nemoto, Y. Fujii, A. Izuoka, M. Kaneko, *J. Jap. Sol. Energy Soc.* 192 (2009) 55.